Sexually Dimorphic Patterns of Episomal rAAV Genome Persistence in the Adult Mouse Liver and Correlation With Hepatocellular Proliferation

Allison P Dane[1], Sharon C Cunningham[1], Nicole S Graf[2] and Ian E Alexander[1,3]

[1]Gene Therapy Research Unit, Children's Medical Research Institute and The Children's Hospital at Westmead, Westmead, New South Wales, Australia; [2]Histopathology Department, The Children's Hospital at Westmead, Westmead, New South Wales, Australia; [3]Discipline of Paediatrics and Child Health, University of Sydney, Sydney, New South Wales, Australia

Recombinant adeno-associated virus vectors (rAAVs) show exceptional promise for liver-targeted gene therapy, with phenotype correction in small and large animal disease models being reported with increasing frequency. Success in humans, however, remains a considerable challenge that demands greater understanding of host–vector interactions, notably those governing the efficiency of initial gene transfer and subsequent long-term persistence of gene expression. In this study, we examined long-term enhanced green fluorescent protein (eGFP) expression and vector genome persistence in the mouse liver after rAAV2/8-mediated gene transfer in early adulthood. Two intriguing findings emerged of considerable scientific and clinical interest. First, adult female and male mice showed distinctly different patterns of persistence of eGFP expression across the hepatic lobule after exhibiting similar patterns initially. Female mice retained a predominantly perivenous pattern of expression, whereas male mice underwent inversion of this pattern with preferential loss of perivenous expression and relative retention of periportal expression. Second, these changing patterns of expression correlated with sexually dimorphic patterns of genome persistence that appear linked both spatially and temporally to underlying hepatocellular proliferation. Observation of the equivalent phenomenon in man could have significant implications for the long-term therapeutic efficacy of rAAV-mediated gene transfer, particularly in the context of correction of liver functions showing metabolic zonation.

Received 15 January 2009; accepted 1 June 2009; published online 30 June 2009. doi:10.1038/mt.2009.139

INTRODUCTION

Vectors based on recombinant adeno-associated virus (rAAV) show special promise for liver-targeted gene transfer. Therapeutic benefit has been reported in murine and canine models for a range of metabolic genetic liver diseases,[1–9] and encouraging evidence of therapeutic potential demonstrated in humans with factor IX deficiency.[10] In mice, highly efficient liver-wide hepatocyte transduction is readily achievable following intravenous or intraperitoneal delivery of vector,[11–13] and increasingly efficient transduction of the human liver can be anticipated as novel liver-tropic capsids are identified. Success in the clinic, however, will also require stable long-term transgene expression. Major challenges include avoidance of anticapsid cytotoxic T lymphocyte responses capable of destruction of transduced cells, as reported recently in two separate clinical trials,[10,14] and loss of episomal rAAV genomes as a consequence of hepatocellular proliferation.[15–17] This latter phenomenon poses a particular challenge for the use of rAAV vectors in the growing liver[13,18] but is also likely to result in declining transgene expression in the adult liver over time.

Successful use of rAAV for liver-targeted gene transfer in humans may be further influenced by the route of administration, vector genome configuration (self-complimentary versus single-stranded), promoter selection, and gender of the recipient. Choice of promoter will not only determine the absolute level of transgene expression achieved and specificity for the liver, but also the pattern of transduction across individual hepatic lobules, which are the functional units of the liver (**Figure 1**). This is of particular significance given the phenomenon of metabolic zonation.[19,20] For example, the urea cycle is most active in periportal hepatocytes,[21] and optimally efficient gene transfer for urea cycle defects will require transcriptional targeting of transgene expression to this region. Although not yet subject to focused analysis, the initial pattern of transgene expression achieved across the hepatic lobule may be further modified over time by loss of episomal rAAV genomes as a consequence of ongoing hepatocellular proliferation. Relatively little is known, however, about hepatocellular proliferation outside the liver regeneration context.[22]

In the current study, we set out to examine the persistence of transgene expression in the adult mouse liver after portal vein injection of an rAAV2/8 vector expressing eGFP under the transcriptional control of a previously described liver-specific promoter with a bias toward expression around the central vein (perivenous).[13] Mindful of potential gender effects, the treated cohorts contained equal numbers of male and female mice. As expected, at early time points, both sexes exhibited a predominantly perivenous pattern

Correspondence: *Ian E Alexander, Gene Therapy Research Unit, The Children's Hospital at Westmead, Locked Bag 4001, Westmead, NSW 2145, Australia. E-mail: iana@chw.edu.au*

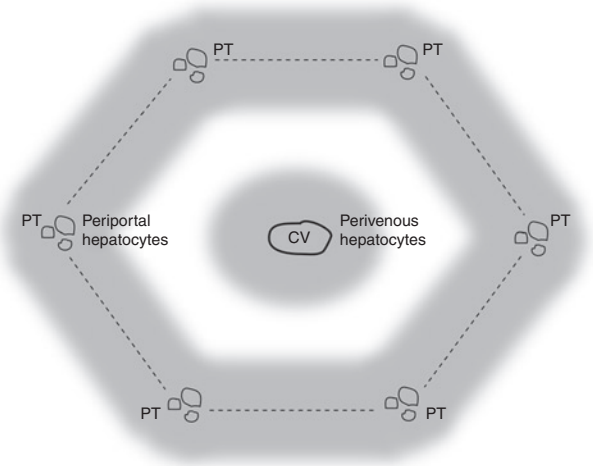

Figure 1 Structure of the murine hepatic lobule. Schematic diagram of a hepatic lobule showing a central vein (CV) and portal triads (PT), which contain branches of the portal vein, hepatic artery, and bile ducts, in the periphery. The boundary of the lobule is circumscribed by dotted lines and the perivenous and periportal zones are indicated by gray shading.

of transgene expression,[13] with overall expression being higher in males, as previously reported.[8,23–28] By 6 months postinjection, there was a falloff in transgene expression in both sexes, but dramatically different patterns of persistence across the hepatic lobule. Female mice maintained a predominantly perivenous pattern of expression, whereas male mice exhibited a distinct inversion of this pattern with marked preferential loss of perivenous transgene expression. This loss of expression correlated with vector genome clearance rather than transcriptional silencing, suggesting a possible link with underlying patterns of hepatocellular proliferation.

Collectively, these novel observations have potential clinical and biological significance. If rAAV vectors prove to show similar sexually dimorphic patterns of transgene persistence and expression in the human liver, their therapeutic efficacy and durability may vary substantially between the sexes depending on the requirement of the therapeutic transgene for expression in perivenous versus periportal zones of the hepatic lobule. Loss of rAAV vector genomes in the adult liver may also prove to be a reliable surrogate marker of hepatocellular proliferation, and, in the context of the current study, the adult mouse has provided unexpected insights into hitherto unknown gender difference in the pattern of hepatocyte proliferation across the hepatic lobule.

RESULTS

Patterns of persistence of rAAV transgene expression across the hepatic lobule are sexually dimorphic

To establish the stability of transgene expression in the mouse liver following rAAV2/8-mediated gene transfer, young adult male and female C57BL/6 mice were injected via the portal vein with the previously described rAAV2/8-LSP1-eGFP vector.[13] Livers were harvested for analysis from groups of three male and three female mice at 2 weeks, 8 weeks, 6 months, and 12 months postinjection. Histological analysis of tissue sections by fluorescence microscopy at 2 weeks postinjection revealed higher levels of eGFP expression around the central vein (perivenous) in both

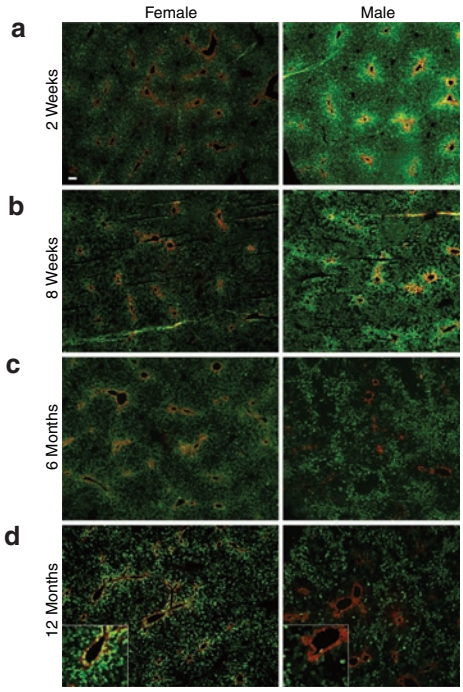

Figure 2 Transgene expression patterns across the hepatic lobule in male and female mice over time. Male and female mice were injected with 1 × 10^{11} vector genomes of rAAV2/8-LSP1-eGFP via the portal vein at 8–10 weeks of age. Liver was harvested at (**a**) 2 weeks, (**b**) 8 weeks, (**c**) 6 months, or (**d**) 12 months postinjection, and 5 µm frozen sections were immunostained with anti-glutamine synthetase antibody to unequivocally identify the central vein (red). Representative photomicrographs (×50 magnification) taken at the same exposure are shown. Bar = 100 µm. Insets in 12-month panels show region immediately adjacent to a central vein (enlarged 2.5-fold).

male and female mice with lower levels in the periportal regions of the hepatic lobule (**Figure 2a**). The only apparent difference between sexes at this early time point was consistently brighter eGFP fluorescence in male mice at equivalent photomicrograph exposures. At 8 weeks, this overall pattern persisted, but with patchy loss of eGFP expression in small clusters of cells becoming evident in both sexes, giving histological sections a "moth-eaten" appearance (**Figure 2b**). By 6 months postinjection, there was a reduction in overall levels of eGFP expression in both sexes, with female mice retaining higher levels of expression in the perivenous region of the hepatic lobule. In male mice, however, there was a distinct inversion of the expression pattern observed at 2 weeks, with marked loss of eGFP expression in the perivenous region and relative preservation of periportal expression (**Figure 2c**). At 12 months, the levels and patterns of eGFP expression across the hepatic lobule appeared to have stabilized, being similar to that observed at 6 months (**Figure 2d**).

To more fully characterize this intriguing sexual dimorphism, we next performed quantitative fluorometry on liver lysates, to better define eGFP expression levels, and quantitative PCR on low molecular weight DNA extracted from bulk liver samples to determine persistence of episomal rAAV vector genomes. Consistent with visual assessment of histological sections, male mice exhibited substantially higher eGFP expression levels at 2 and 8 weeks postinjection, but by 6 and 12 months, expression levels had fallen

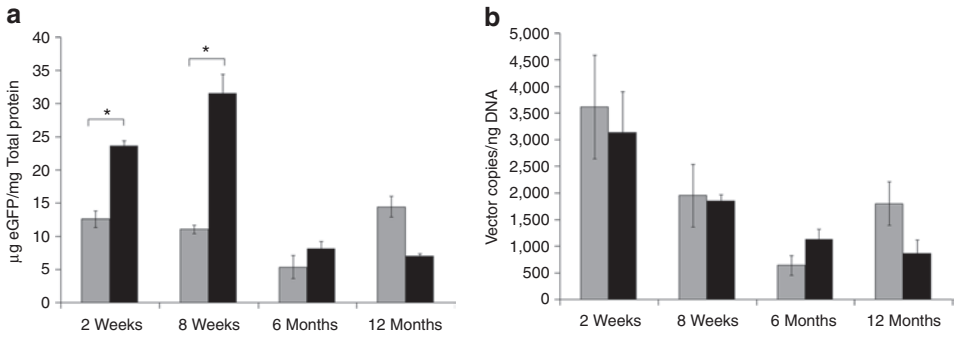

Figure 3 Transgene expression levels and vector genome (vg) persistence in the liver of male and female mice over time. Male and female mice were injected with 1×10^{11} vg of rAAV2/8-LSP1-eGFP via the portal vein at 8–10 weeks of age. Livers from three mice of each sex were harvested at 2 weeks, 8 weeks, 6 months, or 12 months postinjection. Separate pieces of liver from each mouse were used to prepare lysates for (**a**) fluorometric quantitation of eGFP expression and (**b**) for DNA extraction using the Hirt method for Q-PCR quantitation of episomal vg. Background autofluorescence equivalent to 1.6 μg eGFP/mg total protein was subtracted from the fluorescence values presented. Gray and black fill represents means of female and male mice, respectively, ± SEM. *$P \leq 0.05$ using a nonparametric Mann–Whitney *U*-test. eGFP, enhanced green fluorescent protein; Q-PCR, quantitative PCR.

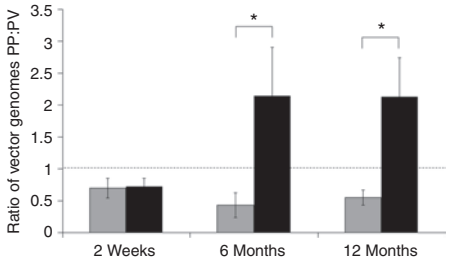

Figure 4 Distribution of vector genomes across the hepatic lobule. Laser capture microscopy (LCM) was used to dissect areas within ~100 μm of central veins and portal triads from frozen liver sections prepared from mice described in the legend of **Figure 2**. Samples were analyzed for total vector genome content (episomal and integrated) by quantitative PCR and normalized against glyceraldehyde-3-phosphate dehydrogenase. Data are presented as the ratio of vector copies detected around the portal triads (PP) and central veins (PV). Gray and black fill represents means of female and male mice, respectively, ± SEM ($n = 3$). Dotted line indicates a ratio of 1. *$P \leq 0.05$ using a nonparametric Mann–Whitney test.

substantially and were within the range of values observed in female mice (**Figure 3a**). Despite this difference in eGFP expression at early time points, analysis of episomal vector DNA from the same livers showed similar levels of vector genome persistence in male and female mice (**Figure 3b**). Comparison of eGFP expression and vector genome levels revealed discordance at both 2 and 8 weeks, particularly in males, with rising eGFP expression levels despite a concurrent decline in vector genome levels. At the later time points of 6 and 12 months, eGFP expression and vector genome levels showed direct correlation in both sexes.

Preferential loss of rAAV genomes in perivenous hepatocytes in male mice correlates with the appearance of sexually dimorphic transgene expression patterns

To begin defining the mechanisms underlying the development of differing eGFP expression patterns across the hepatic lobule in male and female mice, laser microdissection studies were performed to investigate possible differences in vector genome persistence across the hepatic lobule. At 2 weeks postinjection, there was no difference between the sexes in vector genome distribution, with moderately more vector genomes in perivenous than in periportal hepatocytes (**Figure 4**). In female mice, this relative distribution of vector genomes persisted at 6 and 12 months. In distinct contrast, male mice showed a marked preferential loss of vector genomes in perivenous hepatocytes, with relative retention of vector genomes in periportal hepatocytes. Thus, the sexually dimorphic transgene expression patterns established by 6 months of age (**Figure 2**) correlated directly with the underlying patterns of vector genome persistence in the same liver samples.

Given the higher levels of eGFP expression observed in male mice at early time points, we next considered the possibility that eGFP might be exerting a concentration-dependent hepatotoxic effect. To explore this possibility, we measured levels of the liver enzyme alanine aminotransferase in the blood of vector and phosphate-buffered saline (PBS)–injected male and female mice 2 weeks post-treatment. Levels of alanine aminotransferase in vector-injected male (37 ± 1.7 IU/l, $n = 6$) and female (55 ± 13 IU/l, $n = 6$) mice were the same as those in PBS-treated male (36 ± 2.0 IU/l, $n = 3$) and female (52 ± 17 IU/l, $n = 3$) mice. In addition, formalin-fixed, hematoxylin and eosin–stained liver sections from 9 female and 14 male vector-treated mice harvested at intervals ranging from 2 weeks to 12 months after vector exposure were examined by a qualified histopathologist. Sections from four control PBS-treated mice were also examined. The occasional cluster of inflammatory cells was present in five of the 27 mice examined, four were vector-treated (two male and two female) and one PBS control, suggesting no correlation with sex or vector exposure.

Male mice show higher rates of hepatocellular proliferation around the central vein

We next examined hepatocellular proliferation by counting proliferating cell nuclear antigen-positive ($PCNA^+$) cells in multiple histological sections from vector-treated adult male and female mice. At 6 and 12 months after vector delivery, approximately 1 in 400 and 1 in 10,000 hepatocytes stained positive for PCNA, respectively. This is consistent with a marked decline in hepatocellular proliferation during the second 6 months of life and correlates temporally with a stabilization of the pattern and levels of

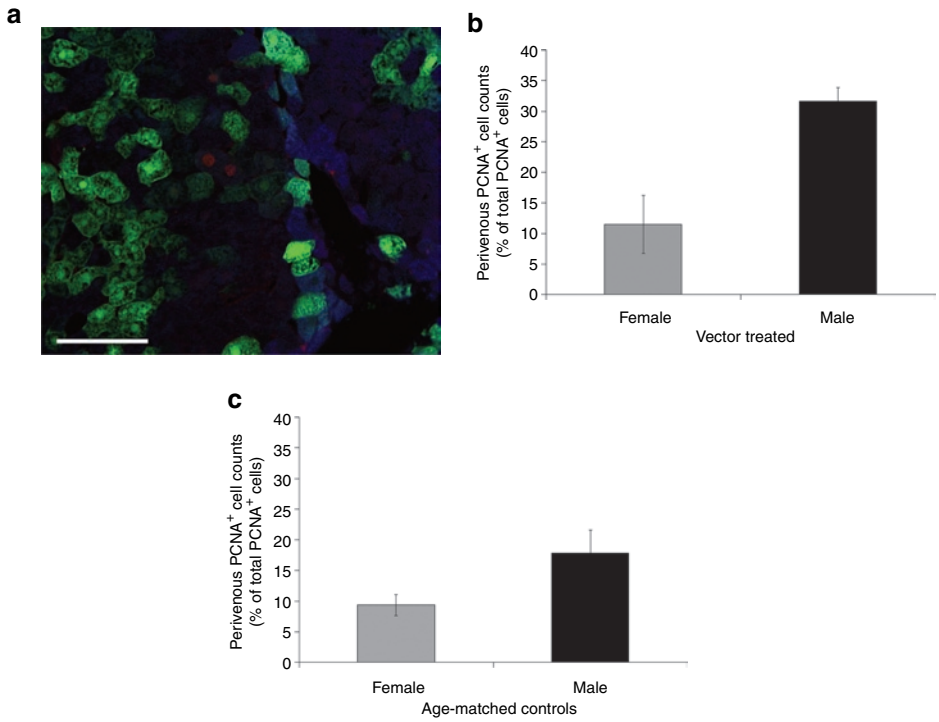

Figure 5 Detection of proliferating cells using PCNA. Liver sections (n = 3 per mouse) from mice 6 months postinjection were immunostained with anti-PCNA to identify proliferating cells and anti-glutamine synthetase antibodies to unequivocally identify the location of the central vein of individual hepatic lobules. (**a**) A representative image (X20/NA0.5) of PCNA (red) and glutamine synthetase staining (blue) cells is shown. The total number of PCNA$^+$ cells per section (76 ± 19.5, mean ± SEM) and proportion within a 100 µm of a central vein in (**b**) vector-treated and (**c**) age-matched control phosphate-buffered saline (PBS)-treated was determined. Gray and black fill represents means of female and male mice, respectively, ± SEM. The difference between vector-treated male (n = 3) and female (n = 3) mice was significant by the Student's t-test (P = 0.034, equal variances not assumed) and nonparametric Mann–Whitney test ($P \leq 0.05$). The difference between age-matched control PBS-treated male (n = 4) and female (n = 4) mice shows the same trend, but did not achieve statistical significance (P = 0.081 and 0.083 by the Student's t-test and nonparametric Mann–Whitney test, respectively). Bar = 100 µm. PCNA, proliferating cell nuclear antigen-positive.

transgene expression observed (**Figures 2** and **3a**). Further analysis of counts obtained at 6 months revealed a trend toward higher absolute proliferation rates in males, but this did not achieve statistical significance (data not shown). However, when we examined the proportion of PCNA$^+$ cells located within 100 µm of the central vein relative to the total number of PCNA$^+$ cells counted in individual vector-treated mice, a distinct difference between the sexes became evident. In male mice, a threefold higher proportion of PCNA$^+$ perivenous hepatocytes was detected (**Figure 5b**). A similar pattern was observed in age-matched control PBS-treated male and female mice (**Figure 5c**), although the difference did not achieve statistical significance. This is the same region where male mice show preferential loss of vector genomes (**Figure 4**), suggesting the mechanistic involvement of hepatocellular proliferation in mediating this effect.

DISCUSSION

In the current study, we examined long-term transgene expression and vector genome persistence in the mouse liver after rAAV-mediated gene transfer in early adulthood. Two intriguing findings emerged of considerable scientific and clinical interest. First, adult male and female mice show distinctly different patterns of persistence of eGFP transgene expression across the hepatic lobule after exhibiting a similar pattern initially. Second, these changing patterns of expression correlated with sexually dimorphic patterns of genome persistence that appear linked both spatially and temporally to underlying hepatocellular proliferation.

Although gender-based differences in transduction performance of rAAV in the liver have previously been reported,[8,23,24,27] those described here are entirely novel and have substantially different implications. These earlier studies report consistently higher levels of transgene expression in male mice at equivalent vector doses that appear to be largely independent of capsid pseudoserotype. The underlying mechanisms have not yet been fully dissected. In the first published study, the livers of male mice were reported to contain higher levels of vector DNA at equivalent doses of an rAAV2/2 vector, with intersex differences mediated through an androgen-dependent pathway.[23] Male mice also exhibited higher levels of nuclear protein binding to the rAAV inverted terminal repeats, possibly indicating differences in the intracellular processing and fate of the vector genome. In a subsequent study using rAAV2/8, vector genome copy number in the liver was reportedly similar in male and female mice despite higher transgene expression levels in males.[8] Our own data obtained 2 and 8 weeks following administration of an rAAV2/8 vector is confirmatory of this latter observation with equivalent levels of vector DNA in male and female livers despite higher eGFP transgene expression in males (**Figure 3**). This discordance, most evident at 8 weeks, between the amount of vector genome in the liver and transgene expression levels in males and females, provides further

evidence for a postcell entry mechanism. More rapid conversion of input single-stranded vector DNA to transcriptionally active double-stranded forms in males is a plausible mechanism. This is made less likely, however, by the recent demonstration that self-complimentary adeno-associated virus vectors, that become competent for transcription without the need for conversion to double-stranded forms, also express more highly in males.[29]

Our novel observation of sexually dimorphic patterns of vector genome persistence and expression across the hepatic lobule only became evident as a consequence of following transgene expression out to 6 and 12 months after vector delivery. Interestingly, by this time, there was no substantial difference between the sexes in the overall levels of transgene expression or corresponding levels of vector genome persistence. From a gene therapy perspective, the potential clinical significance of our observations arise from the fact that a significant number of liver functions show metabolic zonation across the hepatic lobule.[19,20] For example, hepatocytes in the periportal zones are primarily responsible for ureagenesis and gluconeogenesis, and have a high capacity of amino-acid uptake and catabolism, whereas hepatocytes in the perivenous region perform functions such as glycolysis and ketogenesis. Attempts to repair genetic defects in these metabolic pathways by liver-targeted gene transfer will require both efficient targeting of transgene expression to the appropriate zones of the hepatic lobule and stable long-term expression. Assuming humans show similar sexually dimorphic patterns of expression and genome persistence, the long-term durability of the therapeutic effect may vary dramatically in a disease-specific and gender-dependent manner, particularly beyond puberty.

In the current study, we also observed a direct correlation between the spatial and temporal pattern of vector genome persistence and transgene expression. This directly implies that declining transgene expression is predominantly the consequence of vector genome loss rather than transcriptional silencing. Based on existing knowledge[13,15–17] and the data presented, we propose that the predominant mechanism is episomal vector genome degradation occurring in concert with hepatocellular proliferation. Three lines of evidence support this. First, small discrete clusters of hepatocytes with loss of transgene expression became evident by 8 weeks after vector delivery (**Figure 2**). This was most easily seen in males because of higher basal levels of transgene (eGFP) expression and is consistent with individual hepatocytes going through short bursts of proliferation involving one to several rounds of cell division. Second, the sexually dimorphic patterns of genome persistence and expression were fully established by 6 months after vector delivery and then stabilized with little further change through to 12 months. This stabilization of expression corresponds directly with a 25-fold decline in the rate of hepatocyte proliferation as judged by PCNA immunostaining. Finally, vector-treated male mice exhibited a significant threefold higher rate of hepatocyte proliferation in the region of the hepatic lobule lying within 100 µm of the central vein (perivenous), and age-matched control PBS-injected mice showed the same trend. This is the same region showing preferential loss of rAAV genomes in male mice. To our knowledge, this is the first evidence in the literature of differing patterns of hepatocellular proliferation in the male and female liver outside the regeneration context, where the overwhelming majority of hepatocyte proliferation studies have been performed.[30]

It remains possible that our results may have been influenced by the use of *eGFP* as a reporter gene, and it will be important to explore whether similar sexually dimorphic patterns are recapitulated with other transgenes. The higher levels of eGFP observed in male mice at early time points, and particularly around the central vein, combined with reports of GFP toxicity[31–33] render the latter a plausible contributory mechanism. Against this, we saw no evidence of overt sex-specific hepatotoxicity as indicated by normal alanine aminotransferase levels in male and female mice at the time of highest eGFP expression, and no correlation between mouse sex and the observation of the occasional cluster of inflammatory cells observed in liver sections from a minority of mice.

Collectively, these unexpected data provide a strong impetus for further, more comprehensive, studies of rAAV vector genome persistence in male and female mice using additional transgenes and more powerful strategies to study hepatocellular proliferation. From a gene therapy perspective, it will also be particularly important to establish whether similar gender differences occur in the primate and human liver given the immense value of this organ as a therapeutic target.

MATERIALS AND METHODS

Vector production and titration. The rAAV2/8-LSP1-eGFP vector used in the current study was produced by triple transfection of HEK 293 cells with plasmids pLSP1-eGFP, p5E18-VD2/8, and pXX6, and titer assigned by real-time quantitative PCR as previously described.[13] The eGFP transgene in this vector construct is under the transcriptional control of human α1-antitrypsin promoter downstream of two copies of the human apolipoprotein E enhancer.

Animal studies. All animal care and experimental procedures were evaluated and approved by an appropriately constituted Animal Care and Ethics Committee. Male and female C57BL/6 mice at 8–10 weeks of age were injected with 1×10^{11} vector genomes of rAAV2/8-LSP1-eGFP via the portal vein. Briefly, mice were anesthetized by intraperitoneal injection with ketamine (100 mg/kg) and xylazine (10 mg/kg) in 0.9% (wt/vol) NaCl, the portal vein exposed through a ventral midline incision, and 50 µl of vector or PBS injected using a Hamilton syringe (Hamilton, Reno, NV) and a 33-gauge needle. After hemostasis was achieved, the abdominal wall was closed and buprenorphine (0.03 mg/kg) injected subcutaneously for postoperative pain relief. Mice were subsequently monitored for signs of ill health and weight loss. For tissue analysis, mice were killed by CO_2 asphyxiation or cervical dislocation. The liver was removed and sections were either frozen directly or fixed in 4% (wt/vol) paraformaldehyde overnight at 4 °C, cryoprotected in 10–30% (wt/vol) sucrose over 3 days, and then frozen in O.C.T. (Tissue-Tek; Sakura Finetek USA, Torrance, CA) in isopentane/liquid nitrogen for storage at −80 °C. Alanine aminotransferase activity in mouse serum was analyzed in a National Association of Testing Authorities —approved clinical laboratory using the VITROS Fusion 5.1 Chemistry System (Ortho Clinical Diagnostics, Beerse, Belgium).

Fluorometric analysis of eGFP expression. For fluorometric analysis, 0.1–0.2 g of liver tissue was homogenized in lysis buffer (0.5% TritonX, 10 mmol/l 4-(2-hydroxyethyl)-1-piperazineethanesulfonic acid, and protease inhibitor cocktail (Roche Diagnostics, Indianapolis, IN)), the total protein content of the lysate measured (DC Protein assay; Bio-Rad, Hercules, CA), and individual samples adjusted to final concentration of 0.5 mg/ml. A standard curve for eGFP concentration was prepared using recombinant eGFP protein (BioVision Research Products, Mountain

View, CA). Equal volumes of samples and standards were loaded into black plastic 96-well plates (PerkinElmer, Boston, MA) and eGFP fluorescence quantitated on a VICTOR³ multilabel reader (PerkinElmer) using an excitation and emission filter set at 485 nm/535 nm.

Hirt DNA extraction and detection of vector in liver lysates. Low molecular Hirt DNA was extracted from liver using modification of a previously described method.[34] Briefly, 20–30 mg of liver was homogenized in 600 µl lysis buffer (10 mmol/l Tris-Cl pH 8.0, 10 mmol/l EDTA, 1% (wt/vol) sodium dodecyl sulfate) and incubated at 37 °C for 30 minutes. The sample was digested with proteinase K (1 mg/ml) at 37 °C for 1 hour. NaCl (5 mol/l) was added to a final concentration of 1 mol/l and the suspension incubated at 4 °C overnight. After centrifugation (13,000 *g* for 45 minutes), DNA in the cleared lysate was extracted using standard phenol/chloroform and ethanol precipitation methods.[35] Episomal vector copy number was determined in 100 ng of Hirt DNA by quantitative PCR using previously described primers and amplification conditions.[13]

Laser capture microscopy and vector genome quantification. Using a laser microdissection system (P.A.L.M. Microlaser Technologies, Bernried, Germany), liver cells lying within ~100 µm of a central or portal vein were collected from frozen liver sections (5 µm). Samples were incubated at 56 °C overnight in digestion buffer (10 mmol/l Tris pH 8.3, 50 mmol/l KCl, 1.5 mmol/l $MgCl_2$, 0.5% (vol/vol) Tween 20, and 20 µg/ml proteinase K), then inactivated at 96 °C for 10 minutes. Vector copy number was determined by quantitative PCR as previously described.[13]

Immunohistochemistry and detection of transgene expression. For simultaneous detection of glutamine synthetase and eGFP, frozen liver sections (5 µm) were permeabilized in methanol, blocked in PBS containing 10% (vol/vol) fetal calf serum and 10% (vol/vol) goat serum, then reacted with a rabbit polyclonal anti-glutamine synthetase primary antibody (1/150 dilution; Abcam, Cambridge, UK). Bound primary antibody was detected with an Alexa Fluor 594 goat anti-rabbit IgG secondary antibody (1/1000 dilution; Invitrogen, Carlsbad, CA) and images captured using the ×5 Leica objective on a Leica DM IRB inverted microscope (Leica Microsystems, Wetzlar, Germany) (filter sets for eGFP excitation BP450-490/emission LP520 and Alexa Fluor 594 excitation BP515-560/emission LP580) and captured with a SPOT camera using SPOT software version 4.0.1 (Diagnostic Instruments, Sterling Heights, MI).

For simultaneous antibody labeling of PCNA and glutamine synthetase, frozen liver sections (5 µm) were permeabilized in methanol, blocked in PBS containing 10% (vol/vol) fetal calf serum and 10% (vol/vol) donkey serum (Sigma-Aldrich, St Louis, MO), reacted with a rabbit polyclonal anti-glutamine synthetase primary antibody (1/150 dilution; Abcam) for 1 hour, washed and then incubated with 7-amino-4-methylcoumarin-3-acetic acid–conjugated donkey anti-rabbit IgG secondary antibody (1/100 dilution; Jackson ImmunoResearch, West Grove, PA) for 1 hour. After further washing, sections were again blocked with PBS containing 10% (vol/vol) fetal calf serum and 10% (vol/vol) donkey serum before being reacted with a goat polyclonal anti-PCNA primary antibody (1/150 dilution; Santa Cruz Biotechnology, Santa Cruz, CA). This primary antibody was detected with a Texas Red conjugated donkey anti-goat IgG secondary antibody (1/300 dilution; Jackson ImmunoResearch).

Counting PCNA-positive hepatocytes. Three 5 µm liver sections per mouse were analyzed for $PCNA^+$ hepatocytes. After immunolabeling with anti-PCNA and anti-glutamine synthetase antibodies, sections were analyzed using an Olympus BX51 fluorescent microscope and Olympus objectives ×10/NA 0.3 and ×20/NA 0.5 (Olympus, Center Valley, PA). Images were captured with a SPOT enhanced camera using SPOT software version 4.0.1. PCNA staining was detected using an HQ560/55 excitation and HQ645/75 emission filter set (Chroma Technology, Rockingham, VT), eGFP detected using a D480/30x excitation and D535/40m emission filter set (Chroma Technology), and glutamine synthetase detected using a D350/50x excitation D460/50m emission filter set (Chroma Technology). The total numbers of $PCNA^+$ hepatocytes, judged morphologically, were counted across three sections for each of three female and three male mice at 6 and 12 months postinjection. The proportion of $PCNA^+$ hepatocytes ≤100 µm from a central vein (perivenous) clearly delineated by anti-glutamine synthetase immunolabeling was also determined. The number of $PCNA^+$ events per 1,000 hepatocytes was calculated based on the average number of hepatocytes in three SPOT images of known area per mouse and the total area of the histological sections from which the total $PCNA^+$ hepatocyte count was obtained.

ACKNOWLEDGMENTS

We thank Nelson Fausto (University of Washington, Seattle, WA) for helpful discussion of our data and the subject of hepatocellular proliferation, Margot Latham (The Children's Hospital at Westmead) for assistance in manuscript preparation, and Grant Logan and Samantha Ginn for critically reviewing the manuscript. This work was supported by a project grant (423400) from the National Health and Medical Research Council of Australia and postgraduate research scholarship (477110) awarded to A.P.D. from the National Health and Medical Research Council of Australia.

REFERENCES

1. Daly, TM, Okuyama, T, Vogler, C, Haskins, ME, Muzyczka, N and Sands, MS (1999). Neonatal intramuscular injection with recombinant adeno-associated virus results in prolonged β-glucuronidase expression *in situ* and correction of liver pathology in mucopolysaccharidosis type VII mice. *Hum Gene Ther* **10**: 85–94.
2. Fraites, TJ Jr., Schleissing, MR, Shanely, RA, Walter, GA, Cloutier, DA, Zolotukhin, I *et al.* (2002). Correction of the enzymatic and functional deficits in a model of Pompe disease using adeno-associated virus vectors. *Mol Ther* **5**(5 Pt 1): 571–578.
3. Beaty, RM, Jackson, M, Peterson, D, Bird, A, Brown, T, Benjamin, DK Jr. *et al.* (2002). Delivery of glucose-6-phosphatase in a canine model for glycogen storage disease, type Ia, with adeno-associated virus (AAV) vectors. *Gene Ther* **9**: 1015–1022.
4. Matalon, R, Surendran, S, Rady, PL, Quast, MJ, Campbell, GA, Matalon, KM *et al.* (2003). Adeno-associated virus-mediated aspartoacylase gene transfer to the brain of knockout mouse for canavan disease. *Mol Ther* **7**(5 Pt 1): 580–587.
5. Oh, HJ, Park, ES, Kang, S, Jo, I and Jung, SC (2004). Long-term enzymatic and phenotypic correction in the phenylketonuria mouse model by adeno-associated virus vector-mediated gene transfer. *Pediatr Res* **56**: 278–284.
6. Lebherz, C, Gao, G, Louboutin, JP, Millar, J, Rader, D and Wilson, JM (2004). Gene therapy with novel adeno-associated virus vectors substantially diminishes atherosclerosis in a murine model of familial hypercholesterolemia. *J Gene Med* **6**: 663–672.
7. Moscioni, D, Morizono, H, McCarter, RJ, Stern, A, Cabrera-Luque, J, Hoang, A *et al.* (2006). Long-term correction of ammonia metabolism and prolonged survival in ornithine transcarbamylase-deficient mice following liver-directed treatment with adeno-associated viral vectors. *Mol Ther* **14**: 25–33.
8. Sun, B, Zhang, H, Franco, LM, Young, SP, Schneider, A, Bird, A *et al.* (2005). Efficacy of an adeno-associated virus 8-pseudotyped vector in glycogen storage disease type II. *Mol Ther* **11**: 57–65.
9. Koeberl, DD, Sun, BD, Damodaran, TV, Brown, T, Millington, DS, Benjamin, DK Jr. *et al.* (2006). Early, sustained efficacy of adeno-associated virus vector-mediated gene therapy in glycogen storage disease type Ia. *Gene Ther* **13**: 1281–1289.
10. Manno, CS, Pierce, GF, Arruda, VR, Glader, B, Ragni, M, Rasko, JJ *et al.* (2006). Successful transduction of liver in hemophilia by AAV-Factor IX and limitations imposed by the host immune response. *Nat Med* **12**: 342–347.
11. Gao, GP, Alvira, MR, Wang, L, Calcedo, R, Johnston, J and Wilson, JM (2002). Novel adeno-associated viruses from rhesus monkeys as vectors for human gene therapy. *Proc Natl Acad Sci USA* **99**: 11854–11859.
12. Nakai, H, Fuess, S, Storm, TA, Muramatsu, S, Nara, Y and Kay, MA (2005). Unrestricted hepatocyte transduction with adeno-associated virus serotype 8 vectors in mice. *J Virol* **79**: 214–224.
13. Cunningham, SC, Dane, AP, Spinoulas, A, Logan, GJ and Alexander, IE (2008). Gene delivery to the juvenile mouse liver using AAV2/8 vectors. *Mol Ther* **16**: 1081–1088.
14. Mingozzi, F, Meulenberg, J, Hui, D, Basner-Tschkarajan, E, de Jong, A, Pos, P *et al.* (2007). Capsid-specific T cell responses in humans upon intramuscular administration of an AAV-1 vector expressing LPL^{S447X} transgene. *Hum Gene Ther* **18**: 991–992.
15. Nakai, H, Yant, SR, Storm, TA, Fuess, S, Meuse, L and Kay, MA (2001). Extrachromosomal recombinant adeno-associated virus vector genomes are primarily responsible for stable liver transduction *in vivo*. *J Virol* **75**: 6969–6976.
16. Conlon, TJ, Cossette, T, Erger, K, Choi, YK, Clarke, T, Scott-Jorgensen, M *et al.* (2005). Efficient hepatic delivery and expression from a recombinant adeno-associated virus 8 pseudotyped α1-antitrypsin vector. *Mol Ther* **12**: 867–875.
17. Grimm, D, Pandey, K, Nakai, H, Storm, TA and Kay, MA (2006). Liver transduction with recombinant adeno-associated virus is primarily restricted by capsid serotype not vector genotype. *J Virol* **80**: 426–439.
18. Wang, Z, Zhu, T, Qiao, C, Zhou, L, Wang, B, Zhang, J *et al.* (2005). Adeno-associated virus serotype 8 efficiently delivers genes to muscle and heart. *Nat Biotechnol* **23**: 321–328.

19. Jungermann, K and Sasse, D (1978). Heterogeneity of liver parenchymal cells. *Trends Biochem Sci* **3**: 198–202.
20. Jungermann, K (1995). Zonation of metabolism and gene expression in liver. *Histochem Cell Biol* **103**: 81–91.
21. Häussinger, D, Lamers, WH and Moorman, AF (1992). Hepatocyte heterogeneity in the metabolism of amino acids and ammonia. *Enzyme* **46**: 72–93.
22. Fausto, N and Campbell, JS (2003). The role of hepatocytes and oval cells in liver regeneration and repopulation. *Mech Dev* **120**: 117–130.
23. Davidoff, AM, Ng, CY, Zhou, J, Spence, Y and Nathwani, AC (2003). Sex significantly influences transduction of murine liver by recombinant adeno-associated viral vectors through an androgen-dependent pathway. *Blood* **102**: 480–488.
24. Mochizuki, S, Mizukami, H, Ogura, T, Kure, S, Ichinohe, A, Kojima, K *et al*. (2004). Long-term correction of hyperphenylalaninemia by AAV-mediated gene transfer leads to behavioral recovery in phenylketonuria mice. *Gene Ther* **11**: 1081–1086.
25. Berraondo, P, Crettaz, J, Ochoa, L, Pañeda, A, Prieto, J, Trocóniz, IF *et al*. (2006). Intrahepatic injection of recombinant adeno-associated virus serotype 2 overcomes gender-related differences in liver transduction. *Hum Gene Ther* **17**: 601–610.
26. Ogura, T, Mizukami, H, Mimuro, J, Madoiwa, S, Okada, T, Matsushita, T *et al*. (2006). Utility of intraperitoneal administration as a route of AAV serotype 5 vector-mediated neonatal gene transfer. *J Gene Med* **8**: 990–997.
27. De, BP, Heguy, A, Hackett, NR, Ferris, B, Leopold, PL, Lee, J *et al*. (2006). High levels of persistent expression of α1-antitrypsin mediated by the nonhuman primate serotype rh.10 adeno-associated virus despite preexisting immunity to common human adeno-associated viruses. *Mol Ther* **13**: 67–76.
28. Jung, SC, Park, JW, Oh, HJ, Choi, JO, Seo, KI, Park, ES *et al*. (2008). Protective effect of recombinant adeno-associated virus 2/8-mediated gene therapy from the maternal hyperphenylalaninemia in offsprings of a mouse model of phenylketonuria. *J Korean Med Sci* **23**: 877–883.
29. Nathwani, AC, Cochrane, M, McIntosh, J, Ng, CY, Zhou, J, Gray, JT *et al*. (2009). Enhancing transduction of the liver by adeno-associated viral vectors. *Gene Ther* **16**: 60–69.
30. Magami, Y, Azuma, T, Inokuchi, H, Kokuno, S, Moriyasu, F, Kawai, K *et al*. (2002). Cell proliferation and renewal of normal hepatocytes and bile duct cells in adult mouse liver. *Liver* **22**: 419–425.
31. Liu, HS, Jan, MS, Chou, CK, Chen, PH and Ke, NJ (1999). Is green fluorescent protein toxic to the living cells? *Biochem Biophys Res Commun* **260**: 712–717.
32. Huang, WY, Aramburu, J, Douglas, PS and Izumo, S (2000). Transgenic expression of green fluorescence protein can cause dilated cardiomyopathy. *Nat Med* **6**: 482–483.
33. Klein, RL, Dayton, RD, Leidenheimer, NJ, Jansen, K, Golde, TE and Zweig, RM (2006). Efficient neuronal gene transfer with AAV8 leads to neurotoxic levels of tau or green fluorescent proteins. *Mol Ther* **13**: 517–527.
34. Hirt, B (1967). Selective extraction of polyoma DNA from infected mouse cell cultures. *J Mol Biol* **26**: 365–369.
35. Sambrook, J, Fritsch, EF and Maniatis, T (1989). *Molecular Cloning: A Laboratory Manual*. Cold Spring Harbor Laboratory Press: Cold Spring Harbor, New York.